

Nuclear lifetime of states in ^{94}Tc and ^{96}Tc via the pulsed-beam, direct-timing technique*

F. D. McDaniel[†] and F. D. Snyder[‡]

Department of Physics and Astronomy, University of Kentucky, Lexington, Kentucky 40506

(Received 28 January 1974)

The mean lifetimes of the 333 keV level in ^{94}Tc and the 119 and 315 keV levels in ^{96}Tc were measured by the pulsed-beam, direct-timing technique. The values obtained for the mean lifetimes are: $\tau(333 \text{ keV}) = 2.2_{-0.3}^{+0.5}$ nsec, $\tau(119 \text{ keV}) = 37.0_{-0.3}^{+0.6}$ nsec, and $\tau(315 \text{ keV}) = 2.9_{-0.2}^{+0.5}$ nsec. The transition strengths are in agreement with those for other transitions in this mass region.

[NUCLEAR REACTION $^{94}\text{Mo}(p, n\gamma)$, $^{96}\text{Mo}(p, n\gamma)$, measured τ ; pulsed-beam, direct-timing, mean lifetime, Ge(Li) detector.]

I. INTRODUCTION

Nuclear lifetimes provide useful information about the character of excited nuclear states. The lifetime, along with the spin, parity, and other spectroscopic information may be used to test various nuclear models.

A technique for measuring lifetimes which has applications in the lifetime range of $10^{-3} > t_{1/2} > 10^{-11}$ sec is the delayed-coincidence method. This method has been reviewed by Schwarzschild and Warburton,¹ and Stelson² and involves the measurement of the time distribution of radiation depopulating a state relative to the time of population. The time of population of the state may be indicated, for example, by a pulsed beam of particles exciting the state via nuclear reactions. The time of depopulation may be signaled by the detection of deexcitation γ radiation. A number of recent lifetime measurements³⁻⁵ have used the pulsed-beam, direct-timing method. This particular application of the delayed-coincidence technique was used in the present experiment.

If the lifetime to be measured is comparable to or less than the experimental time resolution, a reliable value for the lifetime can be obtained only by comparing the time distribution of the delayed γ -ray intensity to that of a prompt (faster than the experimental time resolution) γ ray nearby in energy.⁶ In addition, unless the prompt and delayed γ -ray time distributions are obtained simultaneously, they may be subject to spurious instrumental distortions.⁷

The $^{94}\text{Mo}(p, n\gamma)^{94}\text{Tc}$ and $^{96}\text{Mo}(p, n\gamma)^{96}\text{Tc}$ reactions were used to study the lifetimes of states in ^{94}Tc and ^{96}Tc . The excited states of ^{94}Tc have been studied by McPherson and Gabbard in this laboratory⁸ through the enhancement of neutron and γ -ray

yields from the $^{94}\text{Mo}(p, n)^{94}\text{Tc}$ reaction at isobaric analog resonance. The comparison of these enhancements with statistical model calculations has provided spin-parity assignments for the 333 (2^-) and the 475 keV (3^-) levels and tentative assignments for six others. The β -decay work of Hamilton *et al.*⁹ has indicated a spin-parity assignment of $J^\pi = 6^+$ or 7^+ for the ground state and 2^+ for the first excited state. The $^{92}\text{Mo}(\alpha, d)^{94}\text{Tc}$ experiment of Zisman and Harvey¹⁰ supports the assignment of 7^+ to the ground state of ^{94}Tc . A similar study has been carried out for ^{96}Tc using the $^{96}\text{Mo}(p, n)^{96}\text{Tc}$ reaction.¹¹ Partial level schemes^{8,11} for ^{94}Tc and ^{96}Tc are shown in Figs. 1 and 2.

II. EXPERIMENTAL DETAILS

A proton beam from the University of Kentucky's 6 MV Van de Graaff accelerator was pulsed at a repetition rate of 2 MHz and bunched to a time width of less than 1 nsec by means of a Mobley beam deflection system.^{12,13} The incident proton beam energies were 5.82 MeV for ^{94}Mo and 5.46 MeV for ^{96}Mo . The targets used were in the form of enriched foils of ^{94}Mo (93.7%) and ^{96}Mo (96.8%). The foil thicknesses were approximately 40 keV for 5 MeV protons.

A planar rather than coaxial Ge(Li) γ -ray detector was used to take advantage of its improved timing properties.¹⁴ Since the γ rays of interest were low energy (85–367 keV), a 5 mm thick planar detector gave sufficient detection efficiency. The γ radiations were detected at a flight path of 25 cm and at 90° relative to the incident proton beam direction. γ -ray energy spectra shown in Figs. 3 and 4 were obtained for ^{94}Tc and ^{96}Tc , respectively, with an energy resolution of 1.5 keV

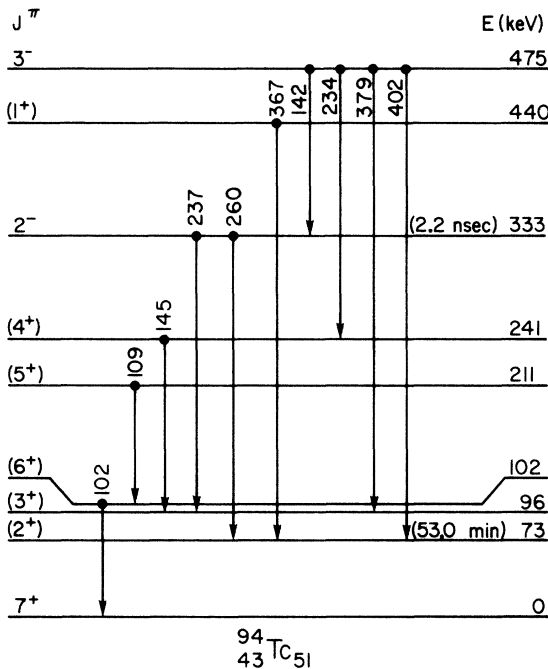


FIG. 1. Energy level diagram of ^{94}Tc .

full width at half-maximum (FWHM) for the 237 keV peak. The γ rays of interest are identified in the figures.

The time distributions of γ radiations were obtained with a time-to-amplitude converter (TAC). The start pulse for the TAC was derived from the output of the Ge(Li) detector. The stop pulse was provided by a suitably delayed inductive beam-pickoff signal. The Ge(Li) detector output signal was processed with an amplitude and rise time compensation method¹⁵ using an ORTEC Model 453 constant fraction timing discriminator (CFTD).¹⁶ The CFTD was adjusted for optimum time resolution for the energy range $50 \leq E_\gamma \leq 1000$ keV. In addition, special care was taken to insure peak

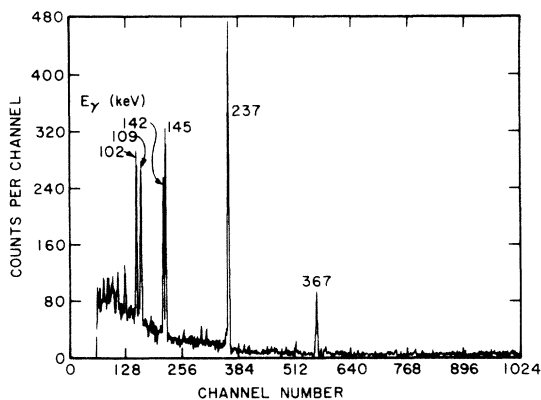


FIG. 3. γ -ray energy spectrum of ^{94}Tc .

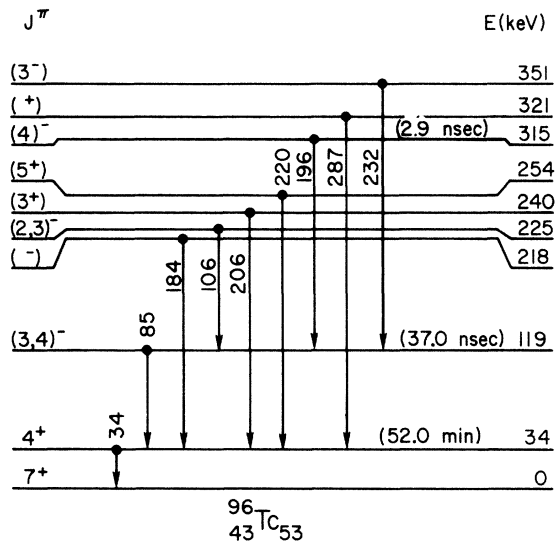


FIG. 2. Energy level diagram of ^{96}Tc .

symmetry of the prompt γ -ray time distributions. The time resolutions obtained (FWHM) are better for higher energy γ rays. The timing circuit was optimally adjusted using the prompt 170 (1 psec)¹⁷ and 842 keV (20 psec)¹⁷ γ rays from the $^{27}\text{Al}(p, p'\gamma)^{27}\text{Al}$ reaction. The 170 and 842 keV time distributions had time resolutions of 4.0 and 1.6 nsec (FWHM), respectively.

Time information for all γ -ray transitions above a lower threshold of 50 keV was processed simultaneously by the timing circuit and then gated into separate sections of the analyzer. The gating signals were logic pulses derived from energy windows placed around the γ rays of interest. This enabled both prompt and delayed γ -ray time spectra to be recorded simultaneously.

The prompt γ rays from ^{94}Tc and ^{96}Tc were identified by comparing their time distributions with the time distributions of the 170 and 842 keV

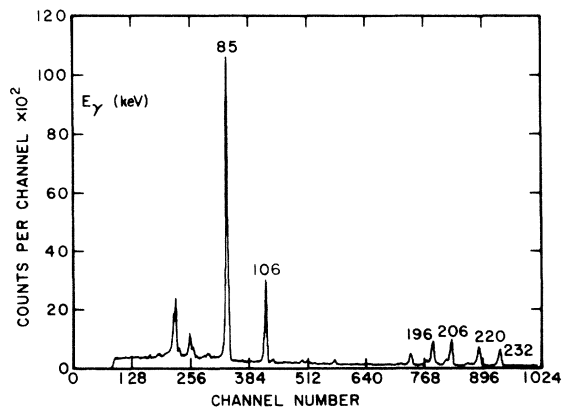


FIG. 4. γ -ray energy spectrum of ^{96}Tc .

TABLE I. Summary of mean lifetimes determined using several techniques of analysis.

Method	E_γ (keV)	Mean lifetime τ (nsec)		
		237	85	196
Slope ^a		2.5 ± 0.4	37.0 ± 0.3	3.2 ± 0.3
Area ^b		$2.4^{+0.6}_{-0.4}$	$37.2^{+1.0}_{-0.9}$	$2.8^{+0.6}_{-0.3}$
2nd moment ^a		$2.1^{+0.6}_{-0.4}$	$36.8^{+0.6}_{-0.4}$	$3.0^{+0.6}_{-0.3}$
3rd moment ^a		$2.1^{+0.6}_{-0.3}$	$37.7^{+0.8}_{-0.6}$	$2.7^{+0.6}_{-0.3}$
Convolved fit ^c		$2.1^{+0.6}_{-0.4}$	$36.3^{+0.8}_{-0.6}$	$3.0^{+0.5}_{-0.2}$
Laplace integral transform ^{a, d}		$2.0^{+0.6}_{-0.4}$	$37.0^{+0.6}_{-0.3}$	$2.8^{+0.6}_{-0.3}$
Adopted value		$2.2^{+0.5}_{-0.3}$	$37.0^{+0.6}_{-0.3}$	$2.9^{+0.5}_{-0.2}$

^a Reference 7.^b Reference 20.^c See text.^d Reference 19.

γ rays from the $^{27}\text{Al}(p, p'\gamma)^{27}\text{Al}$ reaction. This comparison was made between the third moments which reflects the asymmetry of the time distributions. The prompt γ -ray transitions in ^{94}Tc and ^{96}Tc are from states with estimated mean lifetimes of less than 500 psec. Background beneath the peaks in the time distributions was found to be negligible except for the 85 keV transition in ^{96}Tc . The background beneath the 85 keV energy peak was approximated by the average of the backgrounds to either side of the energy peak. The background time distribution was subtracted from the time distribution of the 85 keV γ ray before analysis.

The slope of the time scale was determined by a multiple time mark generator method similar to that used by Bishop.¹⁸ Time marks were generated every 10.0 ± 0.01 nsec.

III. ANALYSIS

The time distributions of γ radiations have been analyzed by a number of standard techniques.^{3,7,19-21} The various methods are listed in Table I with the individual results for all three measured lifetimes. The errors indicated for the various methods reflect both the statistical error and the sensitivity of the method to known systematic variations, such as the γ -ray energy dependence of the centroid and width of the time distribution. The slightly larger positive uncertainties given in Table I for the analysis methods requiring a reference γ ray include the uncertainty in the promptness of the reference γ rays ($\tau_m < 500$ psec). A conventional average weighted by the statistical error of the individual methods cannot be used since the various analysis techniques will have strong cross-correlation coefficients from analyzing the same data.

The slope method fits an exponential to the part of the delayed distribution that is not significantly

affected by the prompt distribution. This method is the one which is least sensitive to the prompt time distribution at the expense of allowing use of only a portion of the delayed distribution. The area method is sensitive to the relative centroid positions and widths of the prompt and delayed distributions. The second- and third-moment methods used were insensitive to the centroid shift. Since the second-moment analysis is a measurement of the time distribution broadening, it is inherently sensitive to the proper width of the prompt time distribution. The third-moment method is a measurement of the relative asymmetry of the prompt and delayed time distributions.

A folding, or convolved, fit was obtained by

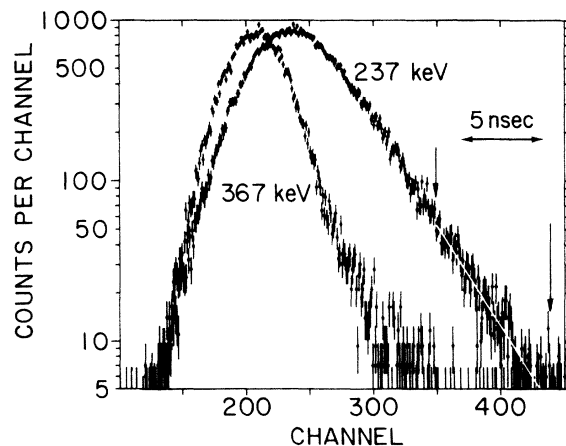


FIG. 5. Time distributions of the 237 and 367 keV γ rays from ^{94}Tc normalized to the same number of counts in the peak channel. The portion of the 237 keV time distribution used in the analysis by the slope method is indicated by the two vertical arrows. The white line represents the calculated time distribution assuming the 237 keV transition is exponentially delayed with a mean lifetime given by the slope technique of 2.5 nsec.

nonlinear least squares fitting an exponential dependence into the prompt time distribution to obtain the delayed time distribution. A χ^2 grid search was made on the mean lifetime and the relative centroid difference between the prompt and delayed peaks. The search on the centroid difference removed the sensitivity of the folding method to this difference. The folding method is only sensitive to the prompt width if the prompt width is comparable to the delayed width.

A. Mean lifetime of the 333 keV (2^-) level in ^{94}Tc

The 237 keV transition in ^{94}Tc was found to be delayed with the mean lifetime of $2.2^{+0.5}_{-0.3}$ nsec. The 142, 145, and 367 keV γ rays were found to be prompt. Therefore, the 475, 241, and 440 keV states in ^{94}Tc are assigned mean lifetimes of $\tau_m < 500$ psec. The time distributions obtained for the 237 and 367 keV γ rays, normalized to the same number of events in the peak channel, are shown superimposed in Fig. 5. Figure 6 is a superposition of the 145 keV prompt distribution and the 237 keV delayed distribution. Neither the 145 nor 367 keV γ ray was close enough in energy to the 237 keV delayed peak to be considered a good prompt representation of the 237 keV time distribution. Therefore, analysis was performed using each separately. The results are shown in Table II. As expected, the analysis techniques that were most sensitive to the time dependences of the centroid and widths upon γ -ray energy, showed the largest variation using the high and low energy prompt peaks. The agreement found, using the shift-corrected, third-moment method, is good between the two possible prompt distributions. This verifies the weak γ -ray energy dependence for the third-moment method.

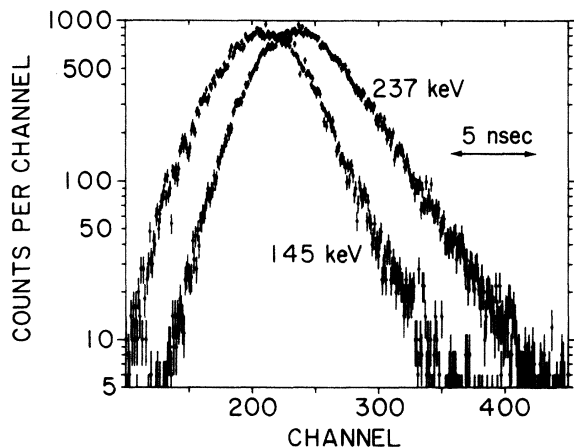


FIG. 6. Normalized time distributions of the 237 and 145 keV γ rays from ^{94}Tc .

TABLE II. Summary of mean lifetimes for the 237 keV delayed transition determined by using the time distributions of the prompt 145 and 367 γ rays.

Method	Mean lifetime τ (nsec)	
	E_γ (keV) (prompt)	367
Area	$2.3^{+0.6}_{-0.4}$	$2.5^{+0.6}_{-0.4}$
2nd moment	$1.8^{+0.6}_{-0.4}$	$2.4^{+0.6}_{-0.4}$
3rd moment	$2.2^{+0.6}_{-0.3}$	$2.0^{+0.6}_{-0.3}$
Convolved fit	$1.7^{+0.6}_{-0.4}$	$2.5^{+0.6}_{-0.4}$
Laplace integral transform	$1.8^{+0.6}_{-0.4}$	$2.2^{+0.6}_{-0.4}$

Cascade feeding to levels which have delayed transitions can be important if the γ rays populating the levels are delayed. For the $^{94}\text{Mo}(p, n)^{94}\text{Tc}$ reaction, the large negative Q value of 5.04 MeV to the ground state insured that cascade feeding would be a very small contribution to the population of the 333 keV level. The prompt 142 keV γ ray was the only observed transition to the 333 keV level and therefore would not contribute to the lifetime.

B. Mean lifetimes of the 315 keV (4^-) and 119 keV ($3, 4^-$) levels in ^{96}Tc

The 196 keV γ -ray transition in ^{96}Tc was delayed with a mean lifetime of $2.9^{+0.5}_{-0.2}$ nsec and the 85 keV γ ray was delayed with a mean lifetime of $37.0^{+0.6}_{-0.3}$ nsec. The 106, 206, 220, and 232 keV γ -ray transitions were found to be prompt. Therefore, the 225, 240, 254, and 351 keV states in ^{96}Tc are assigned mean lifetimes of $\tau_m < 500$ psec.

The normalized time distributions obtained for the 196 and 206 γ rays are shown in Fig. 7. The 206 keV γ ray was used in all analysis requiring

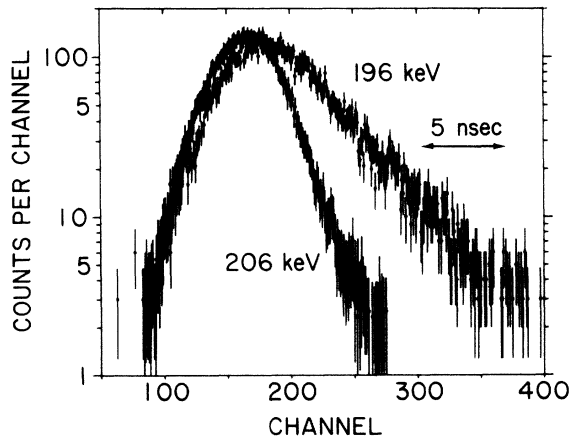


FIG. 7. Normalized time distributions of the 196 and 206 keV γ rays from ^{96}Tc .

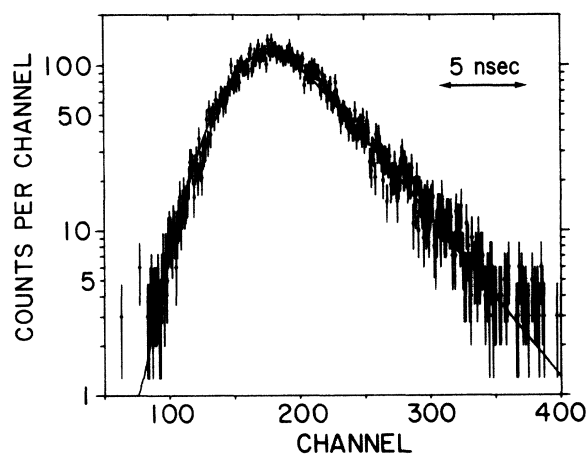


FIG. 8. Time distribution of the 196 keV γ ray from ^{96}Tc . The solid line is the fit to the time distribution using the convoluted fitting method.

a prompt γ -ray time distribution. The 206 keV γ ray was especially suitable because of the small energy difference between the 196 and 206 keV lines. The calculated time distribution for the 196 keV transition determined by using the convoluted fitting method is shown as the solid line in Fig. 8. The fit obtained to the experimental time distribution is very good.

The normalized time distributions obtained for the 85 and 106 keV γ rays are shown in Fig. 9. The 106 keV γ ray was reasonably close in energy and provided a good prompt time distribution. Because the 85 keV transition was appreciably delayed, the slope method was especially applicable. The portion of the 85 keV time distribution used in the analysis by the slope method is shown between the vertical arrows in Fig. 9. The white

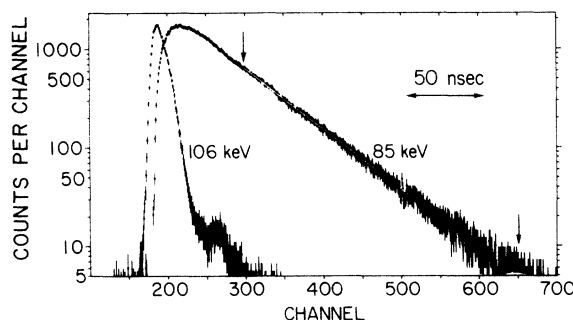


FIG. 9. Normalized time distributions of the 85 and 106 keV γ rays from ^{96}Tc . The portion of the 85 keV time distribution used in the analysis by the slope method is indicated by the two vertical arrows. The white line represents the calculated time distribution assuming the 85 keV transition is exponentially delayed with a mean lifetime given by the slope technique of 37.0 nsec.

line in Fig. 9 represents a calculated time distribution assuming the 85 keV transition is exponentially delayed with a mean lifetime of 37.0 nsec. The results obtained by all methods are in good agreement and are shown in Table I.

Cascade feeding in ^{96}Tc was considered in greater detail since the Q value of the $^{96}\text{Mo}(p, n)^{96}\text{Tc}$ reaction is -3.76 MeV to the ground state of ^{96}Tc . No cascade transitions to the 315 keV level were identified. The population of the 119 keV level is estimated from detector efficiencies to be 25% by direct excitation, 25% from the 196 keV delayed transition, and 50% from the 106 and 232 keV transitions. Higher energy transitions to the 119 keV level were not observed. Both the 106 and 232 keV transitions are prompt and would not contribute to the lifetime of the 119 keV level. The

TABLE III. Transition energies and the experimental and single-particle (sp) estimates of the mean lifetimes. Weisskopf units (W.u.).

	Initial level (keV)	J^π	Final level (keV)	J^π	E_γ (keV)	πL	$\tau(\text{sp})$ (sec)	$\tau(\text{exp})$ (sec)	Strength (W.u.)
^{94}Tc	333	2^-	96	(3^+)	237	$E1$	3.54×10^{-14}		1.6×10^{-5}
						$M1$	2.38×10^{-12}	$2.2^{+0.5}_{-0.3} \times 10^{-9}$	1.1×10^{-3}
						$E2$	4.30×10^{-8}		2.0×10^1
^{96}Tc	315	$(4)^-$	119	$(3, 4)^-$	196	$M1$	4.22×10^{-12}	$2.9^{+0.5}_{-0.2} \times 10^{-9}$	1.4×10^{-3}
						$E2$	1.08×10^{-7}		3.7×10^1
						$E1$	7.58×10^{-13}		2.0×10^{-5}
^{96}Tc	119	$(3, 4)^-$	34	4^+	85	$M1$	5.17×10^{-11}	$37.0^{+0.6}_{-0.3} \times 10^{-9}$	1.4×10^{-3}
						$E2$	7.04×10^{-6}		1.9×10^2
						$E1$			$\sim 0.8 \times 10^{-5}$
Empirical strengths ^a for $A > 40$						$M1$			$\sim 5.0 \times 10^{-3}$
						$E2$			$\sim 1.0 \times 10^2$

^a Reference 23.

effects of the 196 keV delayed transition on the mean lifetime of the 119 keV level are negligible for those results obtained with the slope technique. More than 99% of the feeding occurs before the point in time at which slope analysis of the 85 keV time distribution begins. The portion of the 85 keV time distribution used in the slope analysis is indicated by the vertical arrows in Fig. 9. The contribution of the 196 keV delayed transition to the mean lifetime of the 119 keV level for other techniques of analysis, which are more sensitive to cascading, is believed to be small. This is primarily based upon the good agreement obtained between the slope method and the other techniques of analysis. These results are presented in Table I.

IV. DISCUSSION

Table III presents the transition energies, the experimental mean lifetimes, and single-particle estimates²² of the mean lifetimes. Since the majority of the spin-parity assignments are tentative, single-particle estimates of the mean lifetimes are shown for three possible ($E1$, $M1$, $E2$) multipolarities. The strengths of the delayed transi-

tions in Weisskopf units²³ are in reasonable agreement with each other and also with transitions of other nuclei in this mass region²³ for all three indicated multipolarities. This fact prohibits one from making multipolarity assignments and deducing spins based on the lifetime results alone.

The assumed spin-parity assignments^{8,11} in ^{94}Tc and ^{96}Tc indicate that the 237 keV transition in ^{94}Tc and the 85 keV transition in ^{96}Tc are most likely $E1$ transitions connecting positive and negative parity levels. These positive and negative parity levels can be described partly in terms of $1g_{9/2}$ and $2p_{1/2}$ proton configurations which are l forbidden²⁴ to $E1$, $E2$, $M1$, $M2$, and $M3$ γ -ray decay. The measured strength shows that these low lying levels are not pure configurations but have considerable admixtures of other configurations with more favorable l transfers.

ACKNOWLEDGMENTS

The authors would like to thank F. Gabbard, B. D. Kern, and M. T. McEllistrem for suggesting this problem and for helpful discussions during the course of this experiment.

*Work supported in part by the National Science Foundation.

† Present address: Department of Physics, North Texas State University, Denton, Texas 76203.

‡ Present address: Department of Physics, University of Pittsburgh, Pittsburgh, Pennsylvania 15213.

¹A. Z. Schwarzschild and E. K. Warburton, *Annu. Rev. Nucl. Sci.* **18**, 265 (1968).

²P. H. Stelson, in *Nuclear Research with Low Energy Accelerators*, edited by J. B. Marion and D. M. Van Patter (Academic, New York, 1967), p. 141.

³H. J. Kim and W. T. Milner, *Nucl. Instrum. Methods* **95**, 429 (1971).

⁴B. C. Robertson, G. C. Neilson, and W. J. McDonald, *Nucl. Phys.* **A189**, 439 (1972).

⁵B. C. Robertson, in *Proceedings of the Fifth Symposium of Low-Medium Mass Nuclei, Lexington, Kentucky, 1972*, edited by J. P. Davidson and B. D. Kern (The University Press of Kentucky, Lexington, Kentucky, 1972), p. 225.

⁶A. Schwarzschild, *Nucl. Instrum. Methods* **21**, 1 (1963).

⁷P. Sparrman and F. Falk, *Ark. Fys.* **32**, 447 (1966).

⁸M. R. McPherson and F. Gabbard, *Phys. Rev. C* **7**, 2097 (1973).

⁹J. H. Hamilton, K. E. G. Lobner, A. R. Sattler, and R. Van Lieshout, *Physica* **30**, 1802 (1964); N. K. Aras, E. Eichler, and G. C. Chilosi, *Nucl. Phys.* **A112**, 609 (1968).

¹⁰M. S. Zisman and B. G. Harvey, *Phys. Rev. C* **5**, 1031 (1972).

¹¹F. D. Snyder, K. K. Sekharan, F. Gabbard, and B. D. Kern, *Bull. Am. Phys. Soc.* **18**, 1416 (1973); K. K. Sekharan, F. D. Snyder, F. Gabbard, and B. D. Kern, private communication.

¹²R. C. Mobley, *Phys. Rev.* **88**, 360 (1952).

¹³R. C. Mobley and B. R. Albritton, *Phys. Rev.* **98**, 232 (1955).

¹⁴Z. H. Cho and R. L. Chase, *Nucl. Instrum. Methods* **98**, 335 (1972).

¹⁵R. L. Chase, *Rev. Sci. Instrum.* **39**, 1318 (1968).

¹⁶D. A. Gedcke and W. J. McDonald, *Nucl. Instrum. Methods* **58**, 253 (1968); **55**, 377 (1967).

¹⁷C. M. Lederer, J. M. Hollander, and I. Perlman, *Table of Isotopes* (Wiley, New York, 1968), p. 165.

¹⁸R. J. Bishop, *Nucl. Instrum. Methods* **107**, 9 (1973).

¹⁹P. Sparrman, *Nucl. Instrum. Methods* **41**, 177 (1966).

²⁰T. D. Newton, *Phys. Rev.* **78**, 490 (1950).

²¹Z. Bay, *Phys. Rev.* **77**, 419 (1950).

²²S. J. Skorka, J. Hertel, and T. W. Retz-Schmidt, *Nucl. Data* **A2**, 347 (1966).

²³D. H. Wilkinson, in *Nuclear Spectroscopy*, edited by F. Ajzenburg-Selove (Academic, New York, 1960), Part B.

²⁴A. de-Shalit and I. Talmi, *Nuclear Shell Theory* (Academic, New York, 1963), p. 167.